THE (p,t) REACTION TO POSITIVE PARITY STATES IN ^{165}Er

THE (p,t) REACTION TO POSITIVE PARITY STATES IN ^{165}Er

by

WILLIAM RONALD STOTT, B.Sc.

A Thesis

Submitted to the Faculty of Graduate Studies

in Partial Fulfillment of the Requirements

for the Degree

Master of Science

McMaster University
September, 1974

MASTER OF SCIENCE

McMaster University
Hamilton, Ontario

TITLE: The (p,t) Reaction to Positive Parity States in ^{165}Er

AUTHOR: William Ronald Stott, B.Sc. (Carleton University)

SUPERVISOR: Dr. J.C. Waddington

NUMBER OF PAGES: vii, 43

SCOPE AND CONTENTS:

Positive parity states in ^{165}Er have been studied using the $^{167}Er(p,t)^{165}Er$ reaction. The outgoing tritons were analyzed with a magnetic spectrograph at 13 angles between 6° and 70°. Two 7/2+ states at excitation energies of 63 and 465 keV were populated via $\ell=0$ transitions. Because of the lack of a pronounced minimum in the $\ell=0$ angular distributions, some $\ell\neq0$ strength may contribute to the populating processes. Eight $\ell\neq0$ transitions were seen below 1 MeV excitation energy. A description of the observed positive parity levels has been attempted in the context of a Coriolis coupled Nilsson model calculation.

ACKNOWLEDGEMENTS

I wish to acknowledge the guidance and support of my supervisor Dr. J.C. Waddington. Also, I would like to thank Dr. D.G. Burke and Dr. G. Løvhøiden for their valuable assistance and helpful discussions.

I gratefully acknowledge the assistance given by the Tandem Accelerator personnel for their efficient cooperation during the course of the experiments. Thanks are also due to Mrs. D. Vince and Mrs. M. Dempsey for their careful scanning of the nuclear emulsions, L. Marshall for her skillful drawings, and to Jan Coleman for her speed and accuracy in typing this manuscript. I would like to acknowledge Dr. Z. Preibisz for the valuable lesson he taught me about conducting an experiment.

The work was supported by the National Research Council of Canada while scholarship support was given by McMaster University.

TABLE OF CONTENTS

LIST OF FIGURES

LIST OF TABLES

CHAPTER I

INTRODUCTION

During the past few years a number of studies have been made of the positive parity states of Sm, Gd, Dy, Er, Yb, Hf and W isotopes. In this thesis interest is focussed on the rare earth isotope ^{165}Er. Recent studies of its levels have included the ^{164}Er(d,p)^{165}Er and ^{166}Er(d,t)^{165}Er reactions which were used by Tjøm and Elbek (1969). The high spin states in ^{165}Er have been studied by means of the ^{166}Er(^{3}He,α)^{165}Er (Løvhøiden et al. 1972) and the ^{164}Dy(α,3n)^{165}Er (Hjorth et al. 1969) reactions. The decay of ^{165}Tm into levels of ^{165}Er has also been investigated (Marguier and Chéry 1972).

The positive parity states found are similar to those found throughout the rare earth region which are deformed states arising from the N=6 Nilsson orbitals of the i 13/2 spherical shell model state and the N=4 orbitals of the d 3/2 and s 1/2 states. The model used by Hjorth et al. (1969) to explain the high spin levels that they observed was a simple one which fit the level spacings reasonably well. Nilsson model calculations were made for the 1/2+[660], 3/2+[651], 5/2+[642], 7/2+[633], and 9/2+[624] orbitals which are largely i 13/2 in character. Pairing and Coriolis coupling were then included and a fit to the

observed level spacings was made. Since that time this model has been used throughout the rare earth region. Unfortunately, for the most part only the yrast, or lowest energy band, resulting from this mixture of orbitals has been observed. A more severe test of the model would result if higher bands could be observed.

In this region of the periodic table, there are only three stable nuclei whose ground state is one of these i 13/2 states. They are ^{161}Dy, ^{167}Er and ^{179}Hf. High ground state spins of the target nuclei are desirable since then the high spin states of the residual nucleus would be preferentially populated in the (p,t) two neutron transfer reaction. The positive parity band is really an amalgam of a number of positive parity bands which interact strongly via Coriolis coupling. This interaction is strongest between the high spin states. The isotope ^{167}Er was chosen from the three mentioned above since the (p,t) reaction leaves a residual nucleus of ^{165}Er which has been studied previously in some considerable detail. While the ground state of ^{167}Er is known to be almost pure $IK^{\pi} = 7/2\ 7/2^{+}$ (Kanestrom and Løvhøiden 1971), the lowest i 13/2 band in ^{165}Er is largely K = 5/2 (Hjorth et al. 1969). This means that the ℓ=0 cross section in the (p,t) reaction will not go predominantly to the K = 5/2 band but to the higher lying bands with larger K = 7/2 admixtures.

CHAPTER II

THEORY

2.1 Models

In studying nuclear processes, one is confronted with extremely complex interactions among a large number of nucleons. Even the forces of the interaction between just two nuclear particles are not well understood. Thus, to comprehend what occurs in a nucleus consisting of many particles simplifying assumptions have to be made. To this end, nuclear models have been formulated which allow the physics of the nucleus to be explained. No single nuclear model is successful in completely describing all observed phenomena and so several models exist which are capable of explaining well some phenomenon or some specific region of the periodic table. In the rare earth region, the model most used is that proposed by Nilsson in 1955 (Nilsson, 1955).

Another model of interest in this thesis is one which will describe the scattering processes of beam particles off heavy nuclei. To this end, the optical model for scattering is used in conjunction with the distorted wave Born approximation of quantum mechanics. These models will be discussed briefly in the following two sections. More detailed descriptions of these models can be found

in many nuclear physics texts, such as Preston (1962).

2.2 The Nilsson Model

In the rare earth region, the nuclei are known to have a non-spherical shape since the quadrupole moments of these nuclei are large. As a result of this deformed shape, rotational modes of excitation of the nucleus are possible, with the nucleus rotating about an axis perpendicular to its symmetry axis. Just as spherical nuclei have vibrational modes of excitation so do the deformed nuclei. Vibrational excitation is thought of in terms of a periodic pulsating of the shape of the nucleus. Thus the nuclear level structure may be described with the Hamiltonian

$$H = H_{s.p.} + H_{rot} + H_{vib} + H_{coup}$$

where $H_{s.p.}$ is a modified shell model single particle Hamiltonian describing the motions of the nucleons in their central potential. The term H_{coup} is the coupling among the three modes of motion. If the effect of H_{coup} is small, the nuclear wave function can be written as the product of the eigenfunctions of $H_{s.p.}$, H_{vib} and H_{rot} and the energy level spectrum of the nucleus will be a superposition of the spectra of these three Hamiltonians.

The rotational Hamiltonian has the form

$$H_{rot} = \frac{\hbar^2}{2\mathcal{J}} \tilde{R}^2$$

where $\tilde{R}$ is the angular momentum of the collective motion of the nuclei. The "$\mathcal{J}$" symbol represents the moment of inertia of the nucleus. Consider the equation

$$\tilde{I} = \tilde{R} + \tilde{j} \ .$$

Now, $\tilde{I}$ is the total angular momentum of the nucleus since it is the vector sum of the collective motion rotation and the motion of the nucleons within the potential well. The eigenvalues of this Hamiltonian can be shown to be(Preston 1962)

$$E_{rot} = \frac{h^2}{2\mathcal{J}} [I(I+1) - K^2 + \delta_{K,1/2}(I+1/2)a(-1)^{I+1/2}]$$

where K is the projection of I onto the symmetry axis and a is the decoupling parameter for the K = 1/2 band, which is given by

$$a = - \sum_j (-1)^{j+1/2}(j+1/2)|C_j|^2$$

$|C_j|^2$ is the probability that the total angular momentum of the last odd nucleon is j.

Vibrational excitations can be described in a manner similar to surface vibration in a liquid drop. The Hamiltonian which describes the nucleus when it is vibrationally excited is (Bohr and Mottelson, 1953)

$$H_{vib} = E_o + \sum_{\ell m} H_{\ell m}$$

$$H_{\ell m} = 1/2 \ B_\ell \ |\dot{a}_\ell|^2 + 1/2 \ C_\ell |\alpha_{\ell m}|^2$$

The two terms in the above equation correspond to kinetic and potential energy terms. The coefficient B_ℓ corresponds to the inertial parameter of the nucleus with respect to changes in deformation while the coefficient C_ℓ is a measure of the resistance of the nucleus against deformation.

If the Hamiltonian is quantized such that the $\alpha_{\ell m}$'s represent phonons, the energy levels have the form of the harmonic oscillator

$$E = E_o + \sum_{\ell m} (n_{\ell m} + 1/2)\hbar w_\ell$$

where $n_{\ell m}$ is the number of vibrational phonons in the ℓm mode.

Next is the description of the motion of the individual nuclear particles inside the potential created by all of the nucleons in the nucleus. The most common approach to this problem is to use a model proposed by Nilsson (Nilsson 1955). The nucleons move in a potential shaped like the nucleus containing it. The basic assumption used in this model is that the deformed potential can be described by an anisotropic harmonic oscillator with axial symmetry. This potential is modified by a term proportional to ℓ^2 which in effect broadens the oscillator potential well and has the consequence of depressing the high angular momentum states. The familiar term proportional to $\tilde{\ell}\cdot\tilde{s}$ is also present.

$$H_{s.p.} = \frac{-\hbar^2}{2m} \nabla^2 + \frac{m}{2} (w_\rho{}^2 \rho^2 + w_z z^2) + C\tilde{\ell}\cdot\tilde{s} + D\,\ell^2$$

Depicted in figure 2.1 is the level structure as a function of deformation for single neutron levels for $82<N<126$.

2.3 Band Mixing

As good as the models are there are still discrepancies between experiment and the predictions of the models. In particular is some nuclei significant departures from the I(I+1) rule of the rotational bands occur. Also sometimes strong low multipole transitions occur between bands with greatly different K values. To a great extent these deviations can be understood simply in terms of band mixing.

Consider the effect of coupling two bands of K and K+1. If the levels in these two bands are comparable in energy then the states with the same spins will interact via Coriolis coupling. In effect the levels spread apart so that the lower level is depressed while the upper one is raised. The interaction is an inverse function of the energy separation of the unperturbed levels, thus levels close together separate greatly from one another while distant levels hardly interact at all. There is no coupling between levels of different spin while the coupling between bands of $\Delta K>1$ is very weak. In the mixed positive parity band of ^{165}Er the effect of Coriolis coupling is very significant.

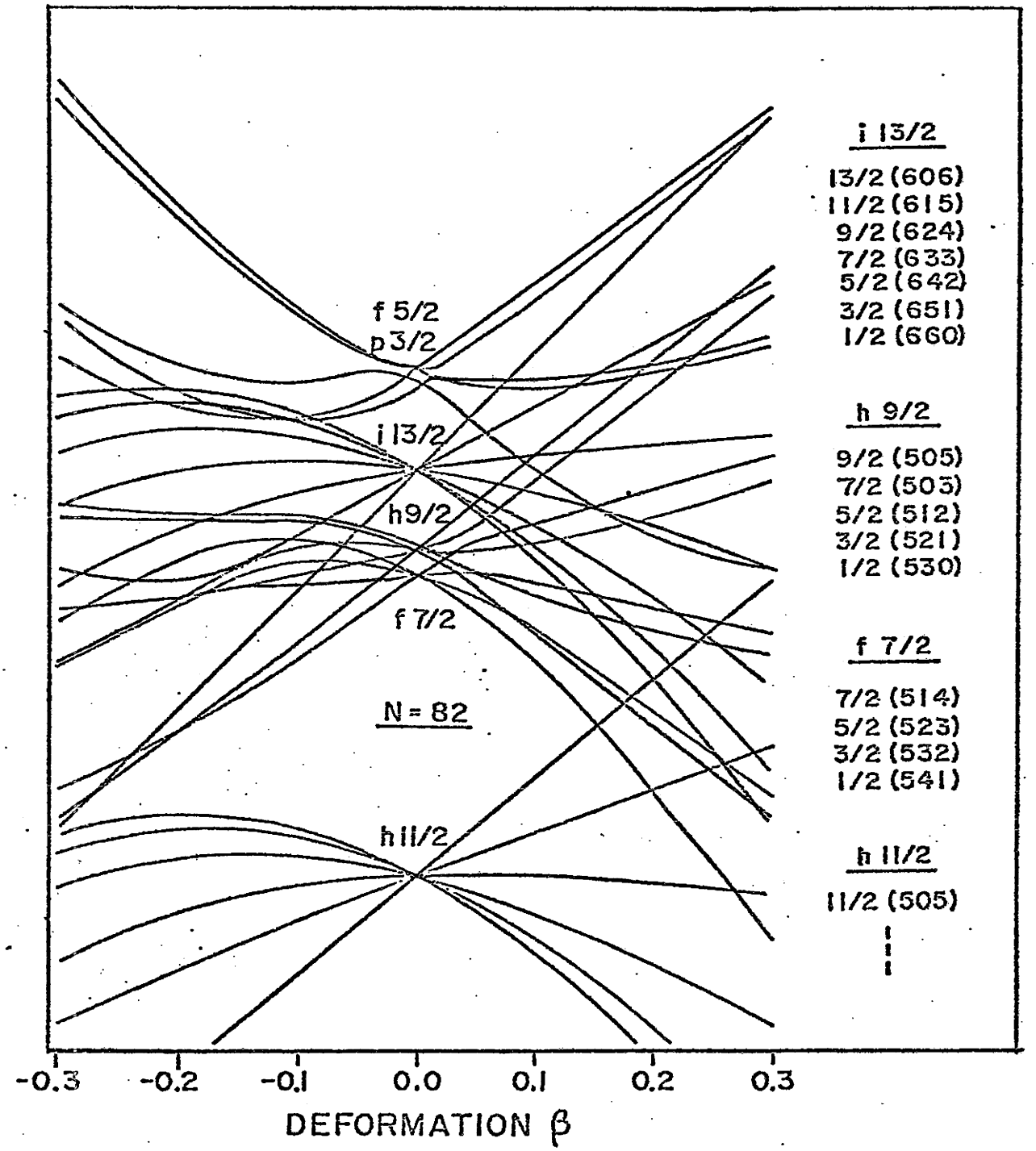

Fig. 2.1

Nilsson diagram for neutron levels in the region N≈90

2.4 DWBA Calculations

In order to calculate the elastically scattered proton cross section and the cross sections for the inelastic (p,t) reactions, it is necessary to use the distorted wave Born approximation. The computer code DWUCK (Kunz, 1967) was used for this purpose.

Optical model potentials are used in the DWBA program. In the optical model, the assumption is made that the projectile particle sees the target nucleus as a "translucent ball". The nucleus is represented as a complex potential where the real part determines the scattering interaction while the imaginary terms take into account the strength of the interaction which tends to absorb the projectile. This is a crude representation to the real situation so that the reaction and scattering cross sections found by such a method will give the gross features of how the cross sections vary, but cannot be expected to reproduce the fine detail of the angular distributions.

For the purposes of the calculations several rather severe approximations have been made. To begin with it was assumed that the nuclear force is a zero range force. Also, it was assumed that in the (p,t) reaction a neutron pair is removed only from a single well defined shell model state. In the calculations made, it was assumed that this

pair of neutrons was removed from the h 9/2 orbital. It turns out, however, that the form of the angular distribution is largely insensitive to which neutron pair is removed (Figure 2.2). Also, despite the fact that ^{165}Er is a deformed nucleus, the shape of the potential used in the calculation was taken to be spherical. The optical model parameters used are those found by Fleming et al. (1970) for the (p,t) reactions on the even tin isotopes. The DX set of parameters was employed here (Table 1). Finally it was assumed that the reaction was a direct single-step process with no channel coupling through the compound nucleus.

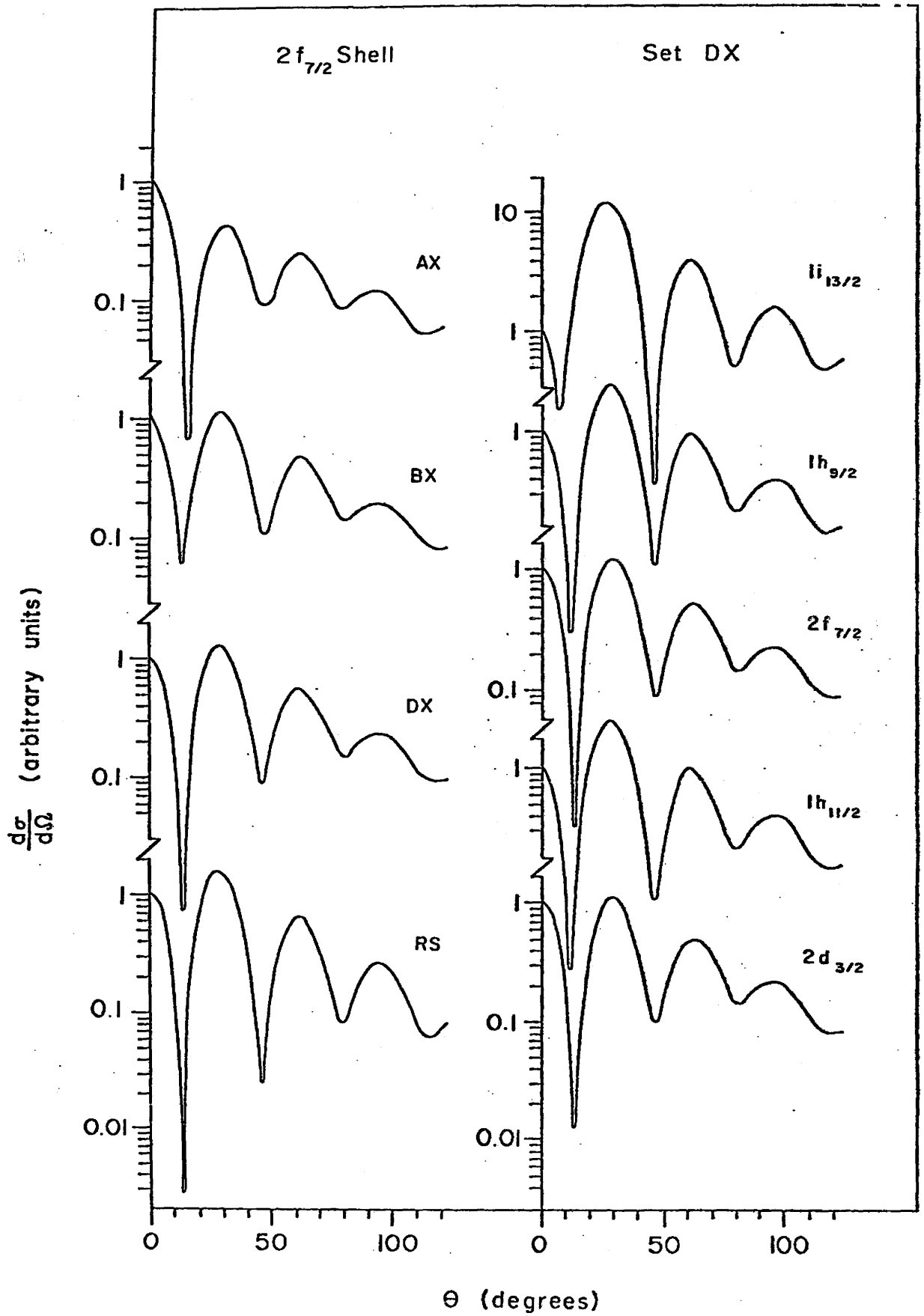

Fig. 2.2

The DWBA distributions for ℓ=0 transitions using different optical model potentials and different neutron shells (from Gadsby 1972).

Table 1

Optical-model parameter sets for DWBA calculations

Channel	Set	V (MeV)	r_V (F)	a_V (F)	W (MeV)	r_W (F)	a_W (F)	W_D (MeV)	r_D (F)	a_D (F)	V_S (MeV)	r_S (F)	a_S (F)	r_C (F)
Proton	A*	46.0	1.33	0.50	9.0	1.33	0.50							1.33
	B*	50.8	1.25	0.65				55.6	1.25	0.47	34.0	1.25	0.65	1.25
	D*	55.7	1.20	0.70				45.2	1.25	0.70	12.0	1.10	0.70	1.20
	R†	57.5	1.17	0.75				40.0	1.32	0.64				1.25
Triton	S†	166.7	1.16	0.75	14.7	1.50	0.82							1.40
	X*	176.0	1.14	0.72	18.0	1.61	0.82							1.14
Bound State		a	1.25	0.65										

* Fleming et al. (1970).

† Maher et al. (1972).

a Adjusted to give two-neutron separation energies of Meredith et al. (1972).

CHAPTER III

3.1 The Experiment

This study was conducted at the McMaster University Tandem Accelerator Laboratory using 16 and 18 MeV protons from the FN Tandem Van de Graaff accelerator. The beam was directed to the Enge split-pole magnetic spectrograph target chamber where it was focussed on an isotopically enriched target of ^{167}Er on a carbon foil backing. Table 2 lists the isotopic impurities and their relative abundances in the target material used. The target itself consisted of 1/4 stone/acre* of target material while the backing had a thickness of 1/3 stone/acre.

The reaction to be studied was the (p,t) two neutron transfer from ^{167}Er into ^{165}Er, where the tritons emitted from the target enter the spectrograph through an aperture as shown in Fig. 3.1. A Si(Li) particle detector was mounted at an angle of 45°,15 cm from the target. It monitored the elastically scattered protons. This monitoring allows for an absolute normalization to be made of the (p,t) differential cross sections as well as indicating the extent of target evaporation throughout the

* 1 stone/acre = 157 $\mu g/cm^2$

Table 2

Isotopic Composition of the ^{167}Er Target

^{170}Er	0.57%
^{168}Er	4.89
^{167}Er	91.1
^{166}Er	3.5
^{164}Er	0.05
^{162}Er	0.01

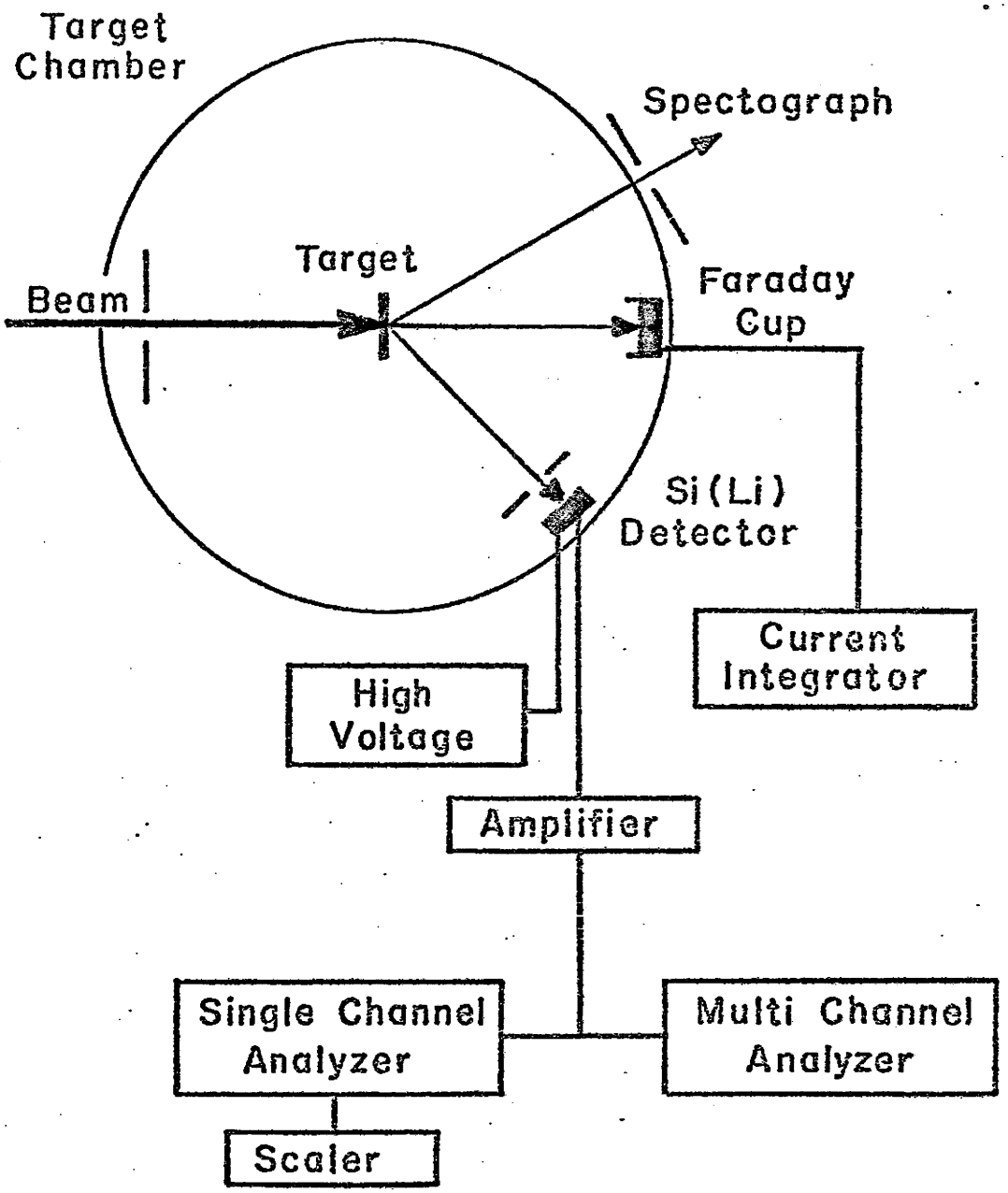

Fig. 3.1

Experiment set-up in the target chamber showing the electronics used.

experiment. Also in the target chamber was a Faraday cup which monitored the beam that passed through the target. The diagram shows the simple electronics used in the experiment. The single channel analyzer had a window set on the pulses from the protons elastically scattered off the erbium while the Nuclear Data 1100 multichannel analyzer accepted all the information on the scattered protons.

The tritons which enter the spectrograph through the 2.6 msr aperture were focussed onto two photographic emulsion plates positioned end to end along the focal plane of the spectrograph. The Enge spectrograph is a second order double focussing high resolution device which focusses particles of identical momentum at the same position along the focal plane. Figure 3.2 shows a top view of the spectrograph. Tritons emitted by the nuclei in a given energy state will be focussed at the same plate position. By observing the peaks on the plates a direct picture of the nuclear level structure was obtained.

The plates used were Eastman Kodak NTB50 nuclear emulsions mounted on glass backing 2 inches wide by 10 inches long. Once developed, the plates were scanned in 1/4 mm strips with a travelling microscope. Exposures were taken at 13 angles from 6° to 70°, each exposure being about 45 minutes in duration. Strips of 0.10 mm thick aluminum absorber were placed in front of the photographic plates

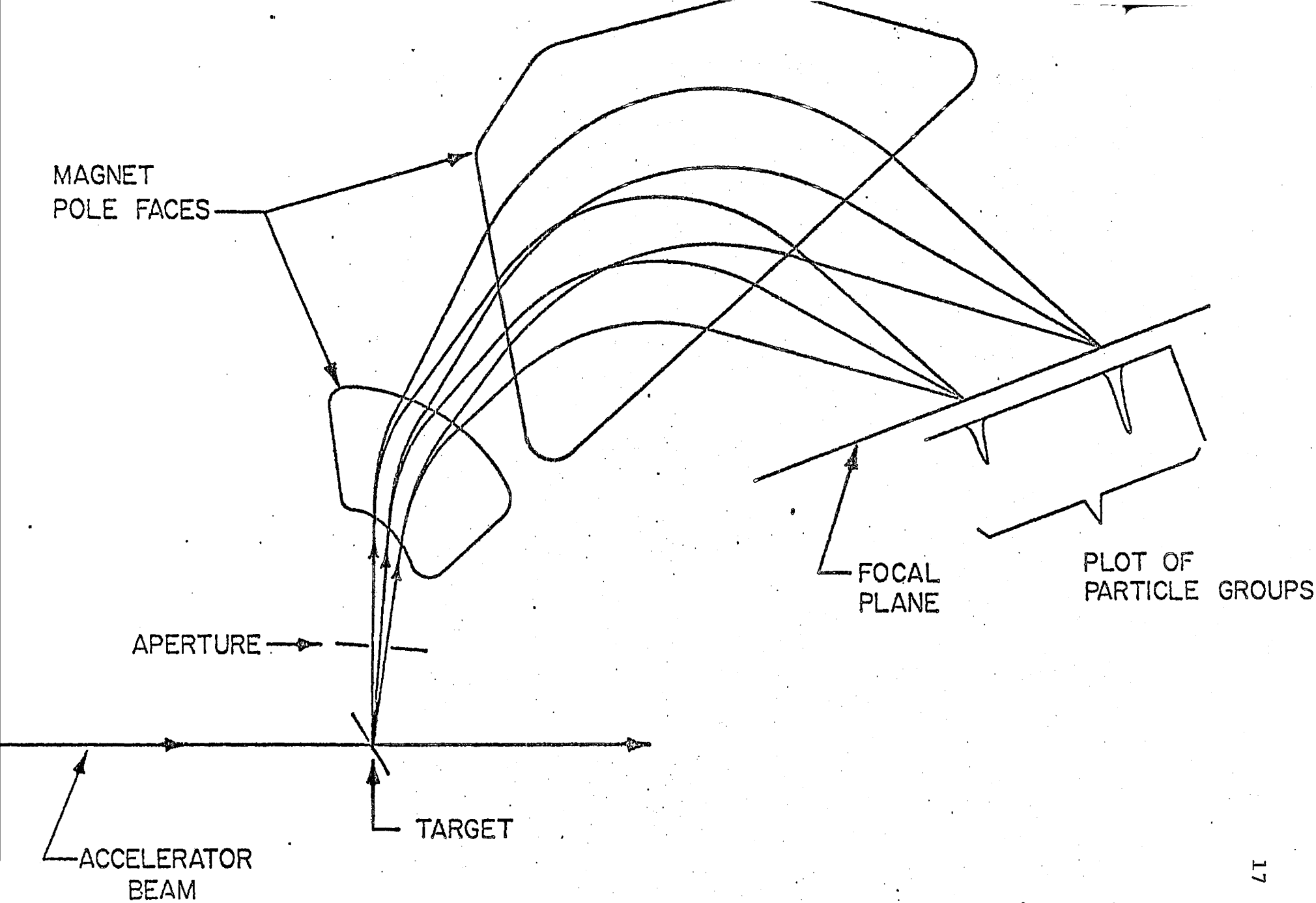

Fig. 3.2

Typical trajectories for particles in the Enge split-pole magnetic spectrograph.

to stop recoiling carbon ions. It is also possible for other light particles such as deuterons or protons to show up on the emulsion. However, for the energy region of interest it is only the deuterons which can create a background, since their momentum can be similar to the tritons. An example of this is the $^{17}O(p,d)^{16}O$ impurity in the 25° spectrum (Figure 3.3). Of course the deuterons will not be focussed properly on the triton focal plane and thus appear as a broad peak especially since the reaction is on a light target. As the angle of observation changes the triton and deuteron peaks move with respect to one another which means that when an angular distribution is taken for the tritons, all the deuteron impurity peaks can be readily identified. Furthermore, since the target material is not 100% pure ^{167}Er, (p,t) reactions on the other erbium isotopes have to be identified. Again Figure 3.3 illustrates this as the tritons for $^{166}Er(p,t)^{164}Er$ form well focussed peaks.

The data for this study were taken in two experiments, one with 16 MeV protons where the angular distributions were obtained and the other with an 18 MeV proton beam. Plates were exposed at 25° and 42.5° with the 18 MeV protons. These angles are those for which the $\ell=0$ transfer cross section is calculated to be a maximum and minimum respectively.

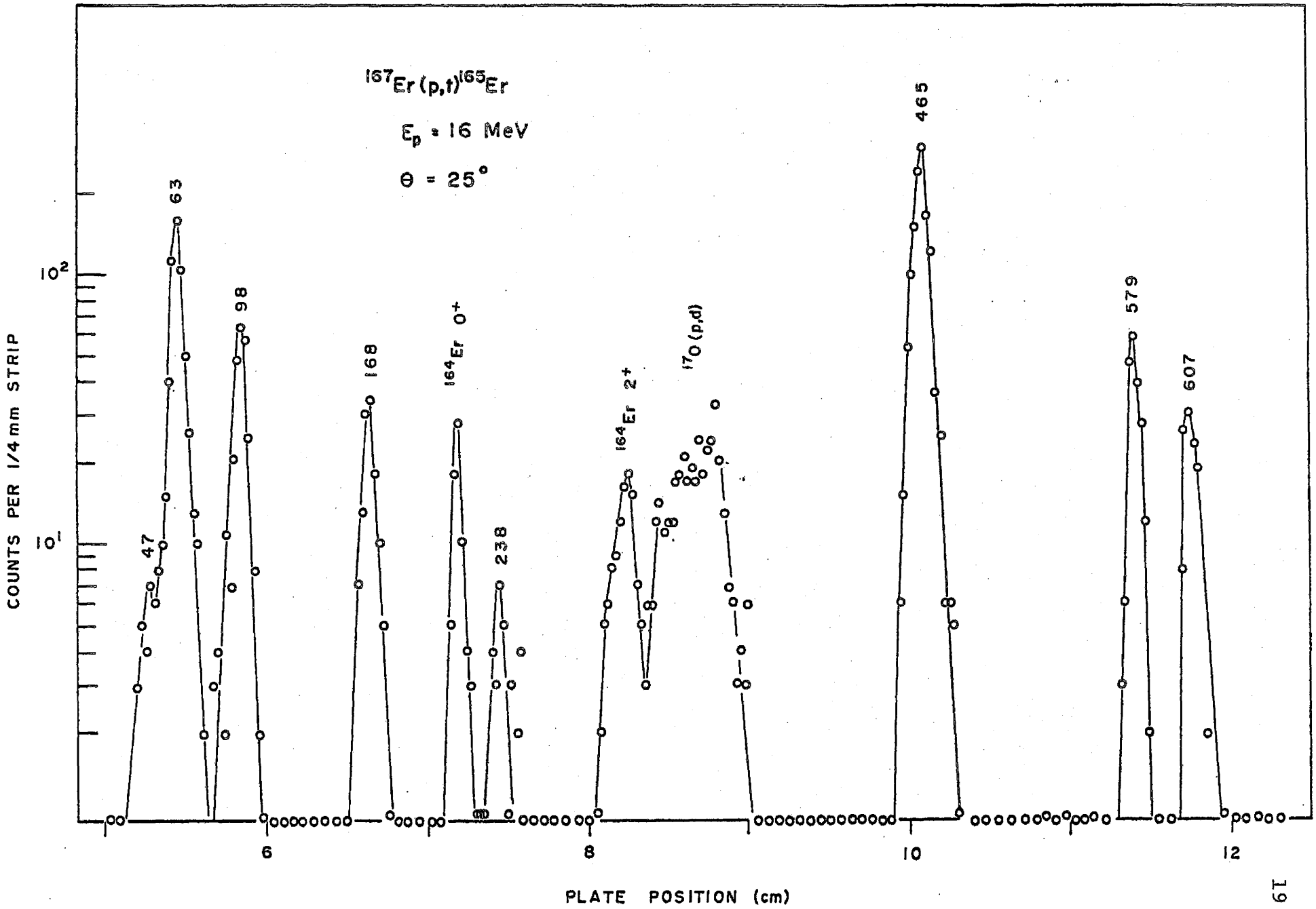

Fig. 3.3
Triton spectra from the $^{167}Er(p,t)^{165}Er$ reaction

The absolute cross sections of the transitions were determined by normalizing their strengths to that of the elastically scattered intensity monitored by the Si(Li) detector in the scattering chamber. The normalizing procedure described by the following formula was used for the 18 MeV data,

$$\frac{d\sigma}{d\Omega}_{\text{spectrograph}} = \frac{d\sigma}{d\Omega}_{\substack{\text{monitor} \\ \text{elastic}}} \times \frac{\Omega_{\text{monitor}}}{\Omega_{\text{spectrograph}}} \times \frac{N_{\text{spectrograph}}}{N_{\text{monitor}}} \times \frac{100}{\%} .$$

The value of $\frac{d\sigma}{d\Omega}_{\substack{\text{monitor} \\ \text{elastic}}}$, was taken to be 489 μb/sr as predicted by the DWBA calculation. The ratio of the solid angles for the monitor counter and the spectrograph was determined from the geometric dimensions of the apertures. The number of protons scattered from erbium in the monitor spectrum is the term N_{monitor}. To correct for the isotopic impurities in the target the percentage of ^{167}Er in the target is included as a factor in the normalization. The absolute cross section accuracy using this procedure should be 20% or better while the relative cross sections for a particular state at different angles should be accurate to better than 10%.

Because of problems with the monitor detector, the normalization of the cross sections was treated in a different manner for the 16 MeV data. A short elastically scattered proton exposure on the plates was used as the basis of the normalization. The same kind of method was

employed as with the other data and so the accuracy of the numbers associated with the 16 MeV data is comparable with 18 MeV data.

3.2 Results

As mentioned previously, angular distributions for the states populated were obtained with a 16 MeV beam of protons. The distributions for the two states with the same spin as the target ^{167}Er, that is 7/2+, are shown in Figure 3.4. Figure 3.4 also shows the angular distribution for the ground state of ^{164}Er. Figure 3.5 shows the angular distributions for states populated by $\ell \neq 0$ processes. An angular distribution for the 374 keV level can not be shown since it was so very weakly populated. In fact, it was only possible to see this weak peak because of the very low background nature of the experiment.

The solid curves shown in Figure 3.4 represent the results of a standard DWBA calculation with the computer code DWUCK for $\ell=0$ angular distributions. The absolute normalization of the calculated distributions has been adjusted to fit the observed strengths. Notice that the minimum in the angular distribution for the ground state of ^{164}Er is very deep and that the DWBA curve fits it very nicely. However, for the two 7/2+ levels in ^{165}Er, the minima, although at the angle predicted for an $\ell=0$ process,

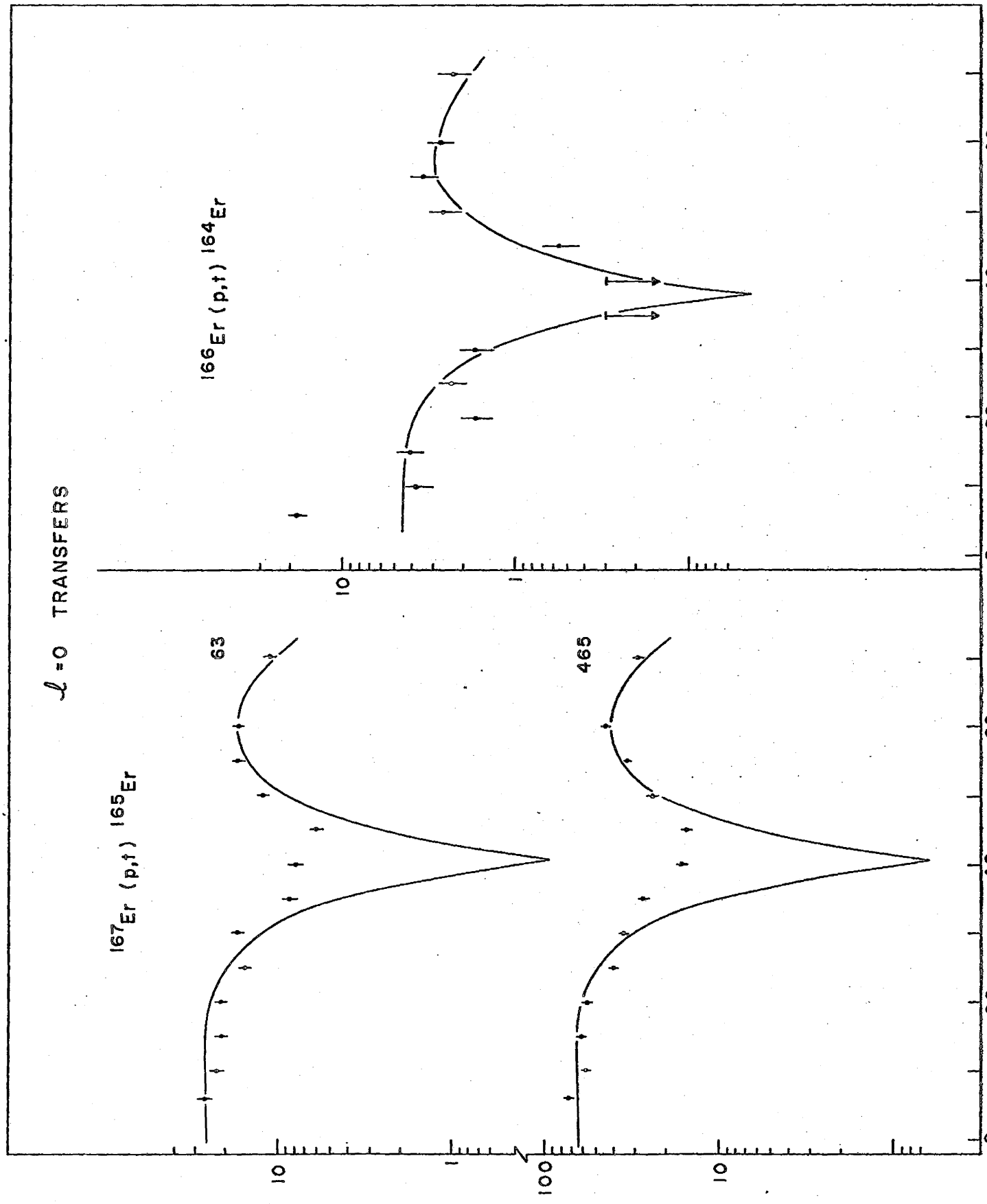
l = 0 TRANSFERS
^{166}Er (p,t) ^{164}Er
^{167}Er (p,t) ^{165}Er
63
465
dσ/dΩ (μb/sr)
10
1
100
0
20
40
60

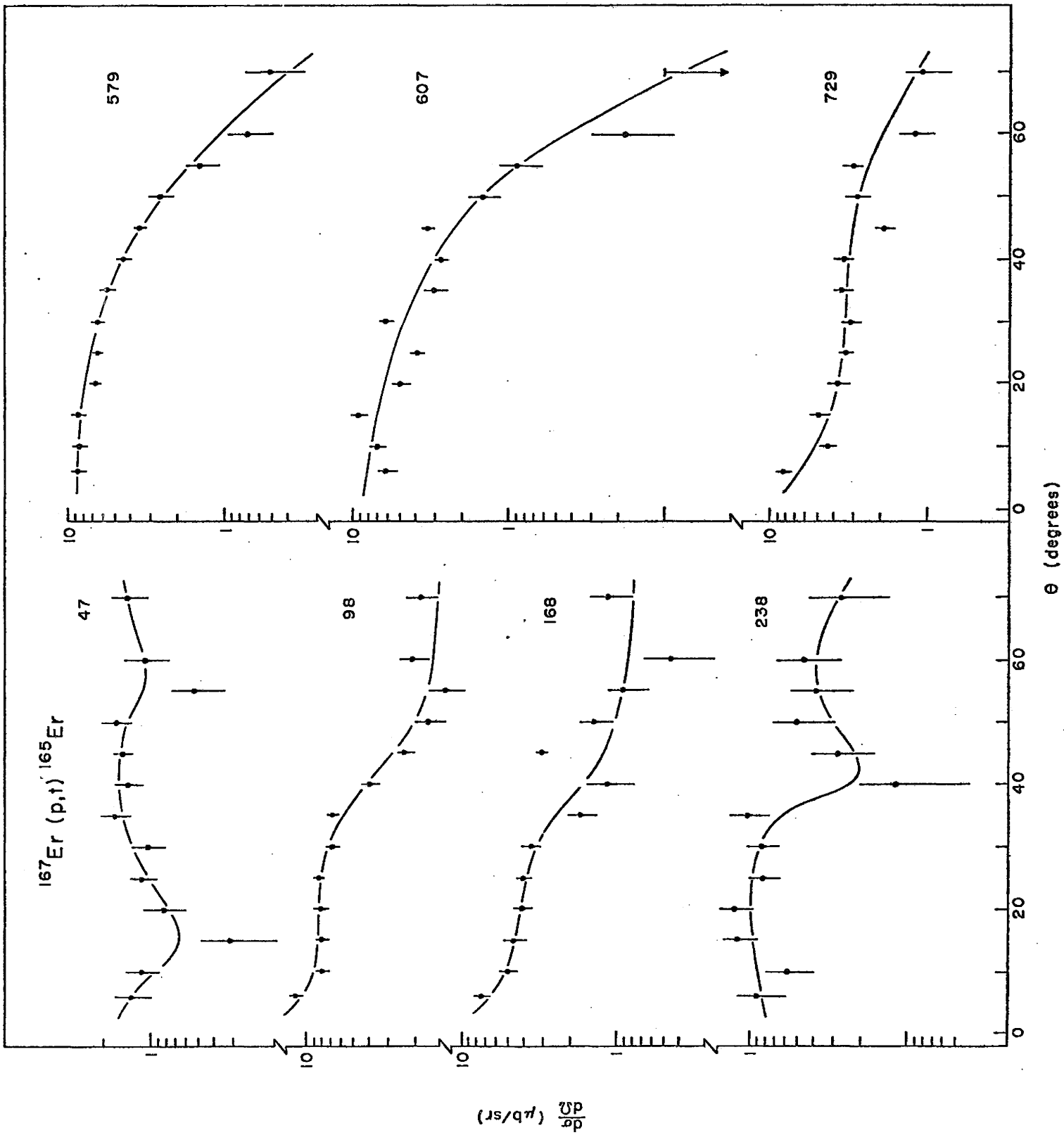
^{167}Er (p,t) ^{165}Er
47
98
168
238
579
607
729
$\frac{d\sigma}{d\Omega}$ (μb/sr)
θ (degrees)

are not nearly as deep as predicted, nor as pronounced as in the $^{166}Er(p,t)^{164}Er$ ground state transition distribution. It was thought that since 16 MeV protons were used that the lack of a good minimum may have been due to a Coulomb barrier effect and so another experiment was conducted using 18 MeV protons. It is known that 18 MeV energy protons give very distinct minima for the (p,t) reaction (Figure 3.6). The 18 MeV spectra taken at 25° and 42.5° are shown in Figure 3.7. Even in that experiment, as in the 16 MeV experiment, the minimum is not as pronounced as a pure ℓ=0 angular distribution exhibits. Energies and cross sections for the levels populated with 18 MeV protons are listed in Table 3.

From the 18 MeV spectra, it can be seen that there are 13 peaks, three of which are from the $^{166}Er(p,t)^{164}Er$ reaction. The total ℓ=0 cross section in this experiment at 25° is approximately 65% of the neighbouring even-even nuclei ℓ=0 cross section as quoted by Oothoudt and Hintz 1973. The 65% of the even-even strength is typical so that it is felt that all of the ℓ=0 strength has been accounted for. Thus there are 10 peaks belonging to ^{165}Er, two of which have been assigned on the basis of the ℓ=0 component in the transitions. The other eight states are not assignable simply from their angular distributions, and so a comparison is made with other experimental results, in particular, the $^{164}Dy(\alpha,3n\gamma)^{165}Er$

Fig. 3.5

Angular distributions for transitions to other levels in ^{165}Er. The curves have no theoretical significance.

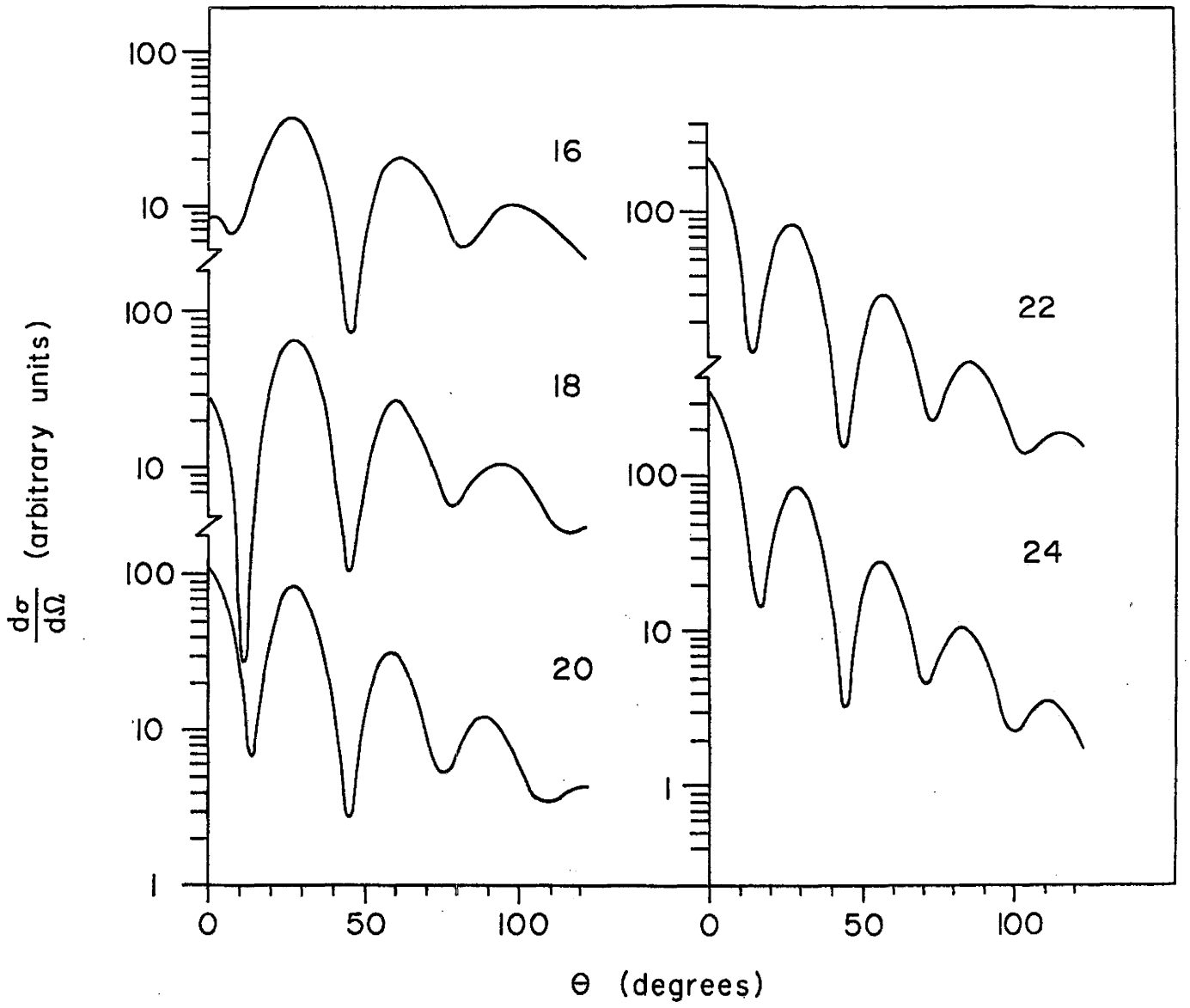

Fig. 3.6

DWBA predicted angular distributions for ℓ=0 transitions from 1h 9/2 state for different beam energies (from Gadsby 1972).

Fig. 3.7

Triton spectra from the $^{167}Er(p,t)^{165}Er$ reaction. The impurity peaks are labelled.

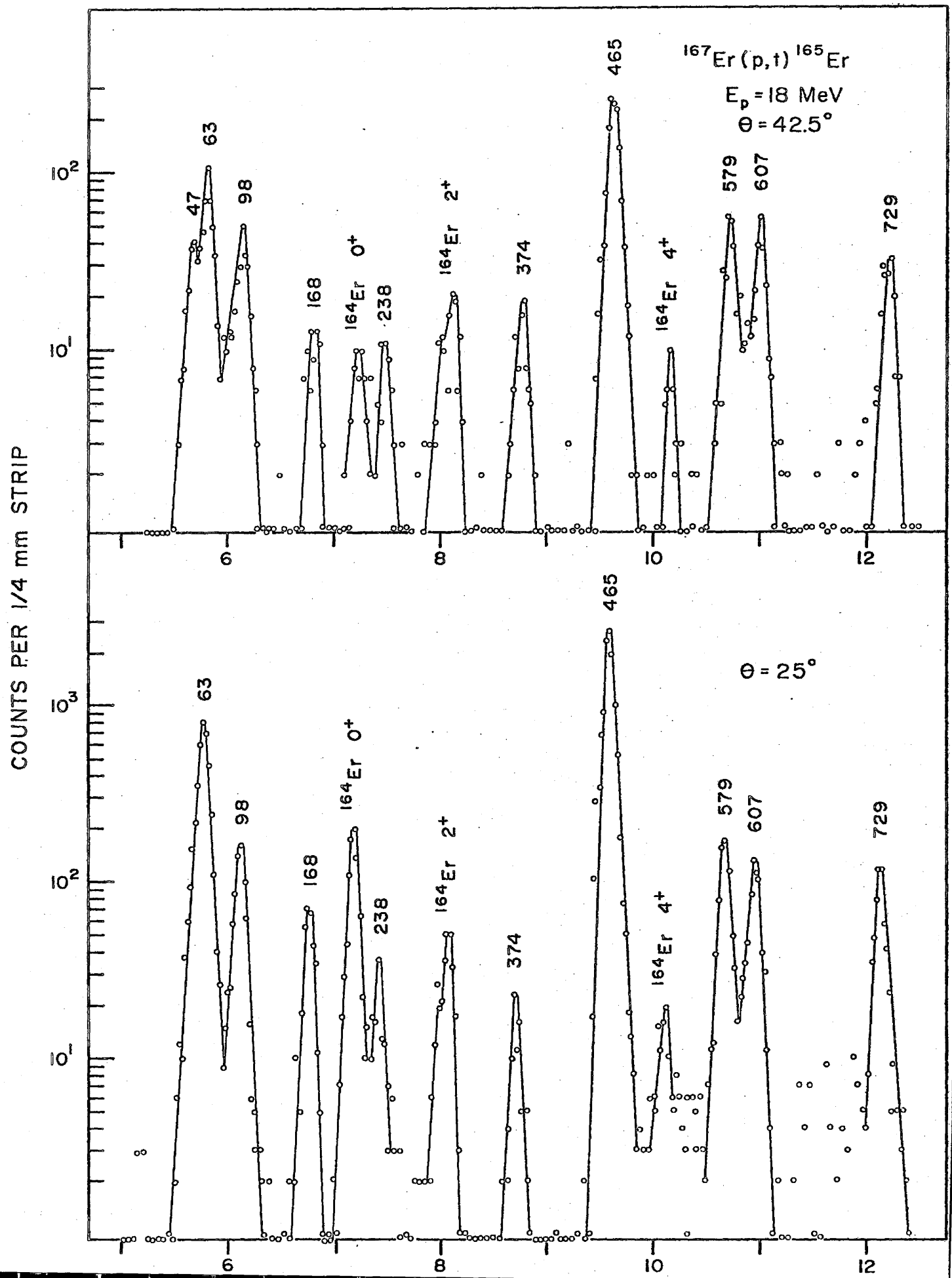
$^{167}Er(p,t)^{165}Er$
$E_p = 18$ MeV
$\theta = 42.5°$
$\theta = 25°$
COUNTS PER 1/4 mm STRIP
10^2
10^1
10^3
47
63
98
168
^{164}Er 0^+
238
^{164}Er 2^+
374
465
^{164}Er 4^+
579
607
729
6
8
10
12

Table 3

Cross Sections for (p,t) transitions to Levels in ^{165}Er. E_p=18 Mev

Energy (keV)	Cross Section (μb/sr) Θ=25°	Θ=42.5°
47	4	4
63	61	12
98	12	7
168	5	2
238	2	1
(296)	<2	<2
372	1	2
465	184	37
581	11	7
607	11	7
730	9	3

work of Hjorth et al. 1969. In Figure 3.8, the levels found in the (p,t) experiment are shown on the left while on the right is shown the level structure of the mixed positive parity band up to spin $19/2^+$ as found by Hjorth et al. 1969. By comparing the energies of the levels observed in the (p,t) and (α,3n) experiments, all but the three highest states can be assigned. These levels are at energies of 579, 607, and 729 keV of which the latter two have previously been seen in the (d,p) work of Tjøm and Elbek 1969. They have not interpreted these two levels.

The strong ℓ=0 transition to the 465 keV 7/2+ level implies that its wavefunction contains a large 7/2 7/2+[633] component since the ground state of the target ^{167}Er is purely 7/2 7/2+[633]. The 9/2+, 11/2+, and 13/2+ members of this band should also be populated in the (p,t) reaction. These may be found among the observed 579, 607 and 729 keV levels, but since the spin values of these states are unknown, definite assignments cannot be made. Since levels at 608 and 728 keV were populated in the (d,p) reaction, it suggests that they are particle states. It would not be unreasonable for the 13/2+ member of the band based on the 465 keV state to be found at 729 keV. If this were so, then one might expect to find this level populated very weakly in the ^{166}Er(^{3}He,α)^{165}Er reaction. In fact, weak peaks have been observed at about this excitation energy in

Fig. 3.8

Comparison of the level structure of ^{165}Er below 1 MeV. The level structure on the left was found with the ^{167}Er(p,t)^{165}Er reaction while on the right is the mixed positive parity band as found by Hjorth et al. 1969. The spins of the levels in the (p,t) experiment were assigned on the basis of the (α,3n) work, except for the 7/2+ levels.

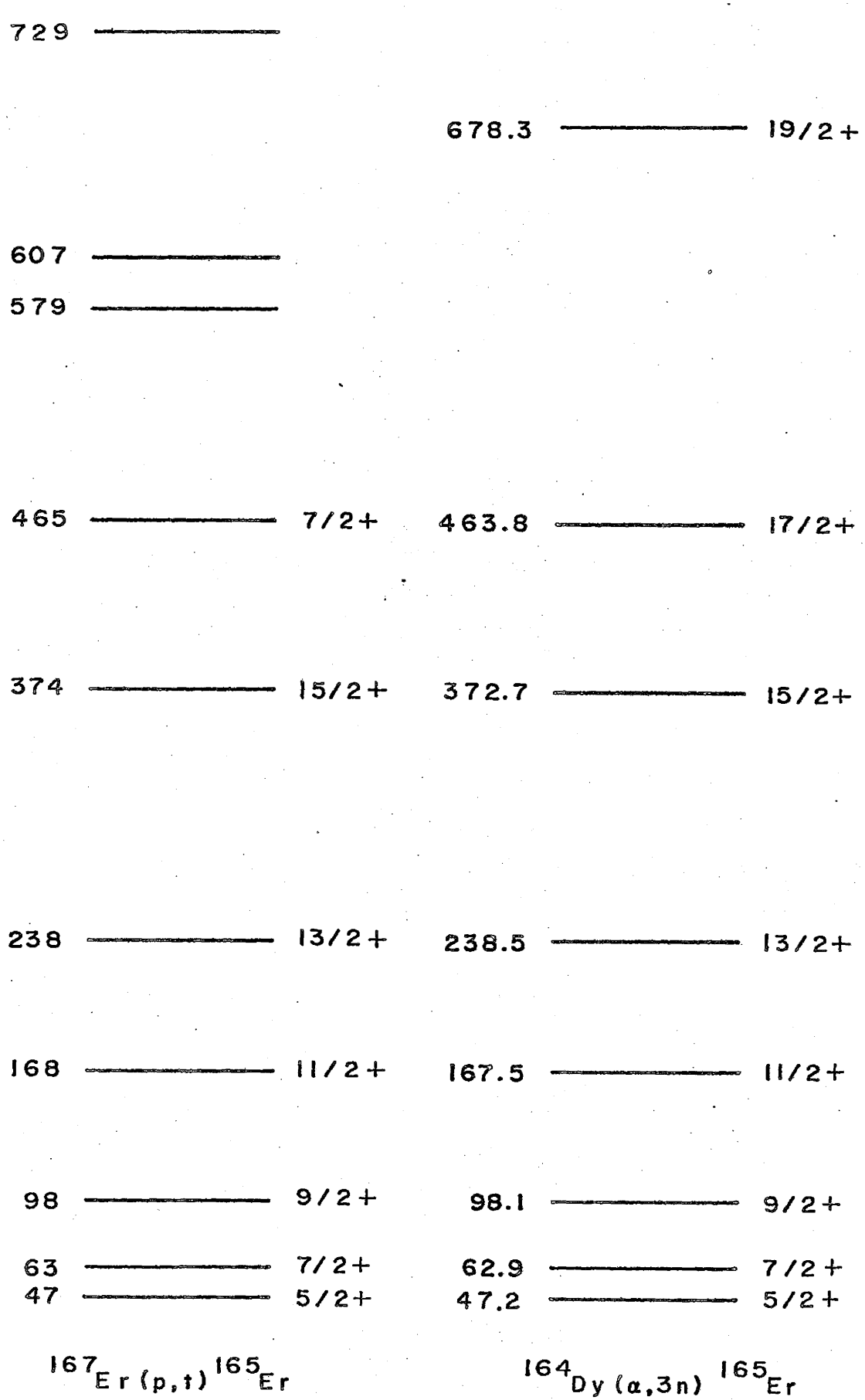
729
607
579
465
7/2+
374
15/2+
238
13/2+
168
11/2+
98
9/2+
63
7/2+
47
5/2+
678.3
19/2+
463.8
17/2+
372.7
15/2+
238.5
13/2+
167.5
11/2+
98.1
9/2+
62.9
7/2+
47.2
5/2+
167Er(p,t)165Er
164Dy(α,3n)165Er

the $^{166}Er(^{3}He,\alpha)^{165}Er$ reaction (Burke, 1974) and the $^{166}Er(d,t)^{165}Er$ reaction (Tjøm and Elbek, 1969). The ratio of intensities in these two experiments is consistent with the state having a high spin.

The measurement of the Q-value of the $^{167}Er(p,t)^{165}Er$ reaction was determined by averaging the values obtained from two different methods. In the first instance, the elastically scattered protons were used to accurately evaluate the beam energy which was then used to calculate the Q-value of the strong 7/2+ 62.9 keV peak. Since the excitation energy of the 7/2+ state is so well known, the ground state Q-value is readily obtained. The second method employed was to use the ground state peak of the isotopic impurity ^{164}Er. Its Q-value is well known so again the beam energy and thus the Q-value of the 62.9 keV state were easily determined. The mean of the values obtained using these two methods gave a ground state Q-value of -6430±5 keV for the reaction $^{167}Er(p,t)^{165}Er$. This number compares favourably with other quoted values in the literature (Table 4).

Table 4

Experiment	Q value (keV)
Meredith & Barber 1972	-6422 ± 5
Oothondt & Hintz 1973	-6427 ± 6
present experiment	-6430 ± 5

CHAPTER IV

4.1 Calculations and Discussions

In attempting to understand the level structure found in the experiment, a calculation is made using the Nilsson model. Though a simple Nilsson model was adhered to without modification of such parameters as the single particle energies and decoupling parameter, pairing and Coriolis coupling were added. Calculations were made for the 1/2+[660], 3/2+[651], 5/2+[642], 7/2+[633] and 9/2+[624] orbitals which are largely i 13/2 in character.

Since ^{165}Er is a permanently deformed prolate nucleus the band structure of the unperturbed levels will have the form

$$E = E_{q.p.} + A_{band}\ (I(I+1) - K^2 + \delta_{K\ 1/2}(-1)^{I+1/2}a(I+1/2))$$

where A_{band} is the inertia parameter which is characteristic of the nucleus. The $E_{q.p.}$ term is the quasi-particle energy upon which the rotational band is built and is given from pairing theory (Preston, 1962) as

$$E_{q.p.} = \sqrt{(\varepsilon_K-\lambda)^2+\Delta^2} - E_o$$

The single particle energies ε_K were calculated from the Nilsson model - given the deformation and the potential

parameters C and D. The symbol λ represents the Fermi energy and Δ is half the energy gap. The ground state quasi-particle energy is denoted by E_o. Effectively then $E_{q.p.}$ is the excitation energy of the band head.

Pairing theory in nuclear physics resulted from the theory of superconductivity as developed by Bardeen, Cooper and Schrieffer (Bardeen et al. 1957). Because of the pairing interaction, the pairs of particles are distributed among the levels in a correlated manner. Thus levels are no longer considered to be either completely filled or completely empty but that the probability of being occupied by a pair is given by V_K^2 while of being unfilled by U_K^2, where

$$U_K^2 = 1/2\left(1 + \frac{(\varepsilon_K-\lambda)}{[(\varepsilon_K-\lambda)^2+\Delta^2]^{1/2}}\right); V_K^2 = 1/2\left(1 - \frac{(\varepsilon_K-\lambda)}{[(\varepsilon_K-\lambda)^2+\Delta^2]^{1/2}}\right).$$

In the absence of a pairing interaction, all those states below the Fermi level are occupied while all the levels above the Fermi level are vacant. With the addition of the pairing force the level occupation is smoothed out so there is no discrete level of occupancy and non-occupancy. The energy at which the occupation probability is 50% is the Fermi level, λ, and the parameter which describes the diffuseness of the Fermi surface is the half energy gap, Δ. This is estimated from the odd-even mass difference in the adjacent nuclei to be about 1 MeV.

In addition to the pairing force, Coriolis coupling has also been added to the theory and is treated as a

perturbation on the Nilsson model potential. The Coriolis matrix elements are given as (Hjorth et al. 1969)

$$V_{K,K+1} = -\alpha\, A_{band} \langle K|j_-|K+1\rangle \sqrt{(I-K)(I+K+1)}$$

$$\times\ (U_K U_{K+1} + V_K V_{K+1}) .$$

Just as A_{band} is considered as a constant for a nucleus so is the α which adjusts the mixing strength. A strong Coriolis mixing manifests itself in a conspicuously small rotational parameter for the lowest energy band and the level spacings, particularly of the higher spin members, resemble a decoupled K=1/2 band.

In carrying out the calculations the parameters that were allowed to vary were A_{band}, α, E_o and λ while other numerical values were obtained directly from the theory. Having initially tried to fit the data with the four parameters as variables, it was found impossible to achieve a good fit at the same time to the energy levels and to the ratio of cross sections for the 7/2+ states. The cross section ratio can be calculated very simply if the wavefunctions of the states are known. The single particle wavefunctions of the lowest 7/2+ states at energies of 59.8 and 473.8 keV as found in the best energy fit calculation corresponding to the 63 and 465 keV levels were calculated to be

$$\psi_{59.8} = 0.043|1/2\rangle + 0.293|3/2\rangle + 0.915|5/2\rangle + 0.274|7/2\rangle$$

$$\psi_{473.8} = -0.056|1/2> -0.265|3/2> -0.195|5/2> +0.943|7/2>$$

The $|1/2>$, $|3/2>$,... refer to the Nilsson orbitals 1/2+[660], 3/2+[651],... The cross section ratio should be as the ratio of the 7/2 intensities since the ground state of the target nuclei is pure $IK^{\pi} = 7/2\ 7/2^{+}$. The ratio from this calculation is $(.943)^2/(.274)^2 = 11.8$. Experimentally the ratio was found to be 4.5.

In an attempt to achieve a better agreement with the data, parameters other than those mentioned above were allowed to vary, but even with the extra variables no better fit was found. Presumably, if enough parameters had been varied then agreement would be achieved but then an explanation in terms of the model would be doubtful. Alternatively, an illustration of how the cross section and energy fits vary with the Fermi level are shown in Figures 4.1 and 4.2. Figure 4.1 shows how the 7/2+ states alter in cross section and energy as the Fermi energy changes. Figure 4.2, on the other hand, is a diagram showing the level structure up to spin 25/2+ as it varies with the Fermi level. The best energy fit to the known energies of the 5/2+ through 25/2+ states is at a Fermi energy 203 keV above the 5/2[642] Nilsson single particle energy, however, the cross section ratio agrees with experiment at a Fermi level approximately 350 keV above the 5/2[642] single particle energy. A likely solution to this dilemma is that other factors such as coupling to vibrational states which have

Fig. 4.1

Variation of the 7/2+ states in intensity and excitation energy with Fermi level. The Fermi level is defined relative to the 5/2+[642] Nilsson model single particle energy.

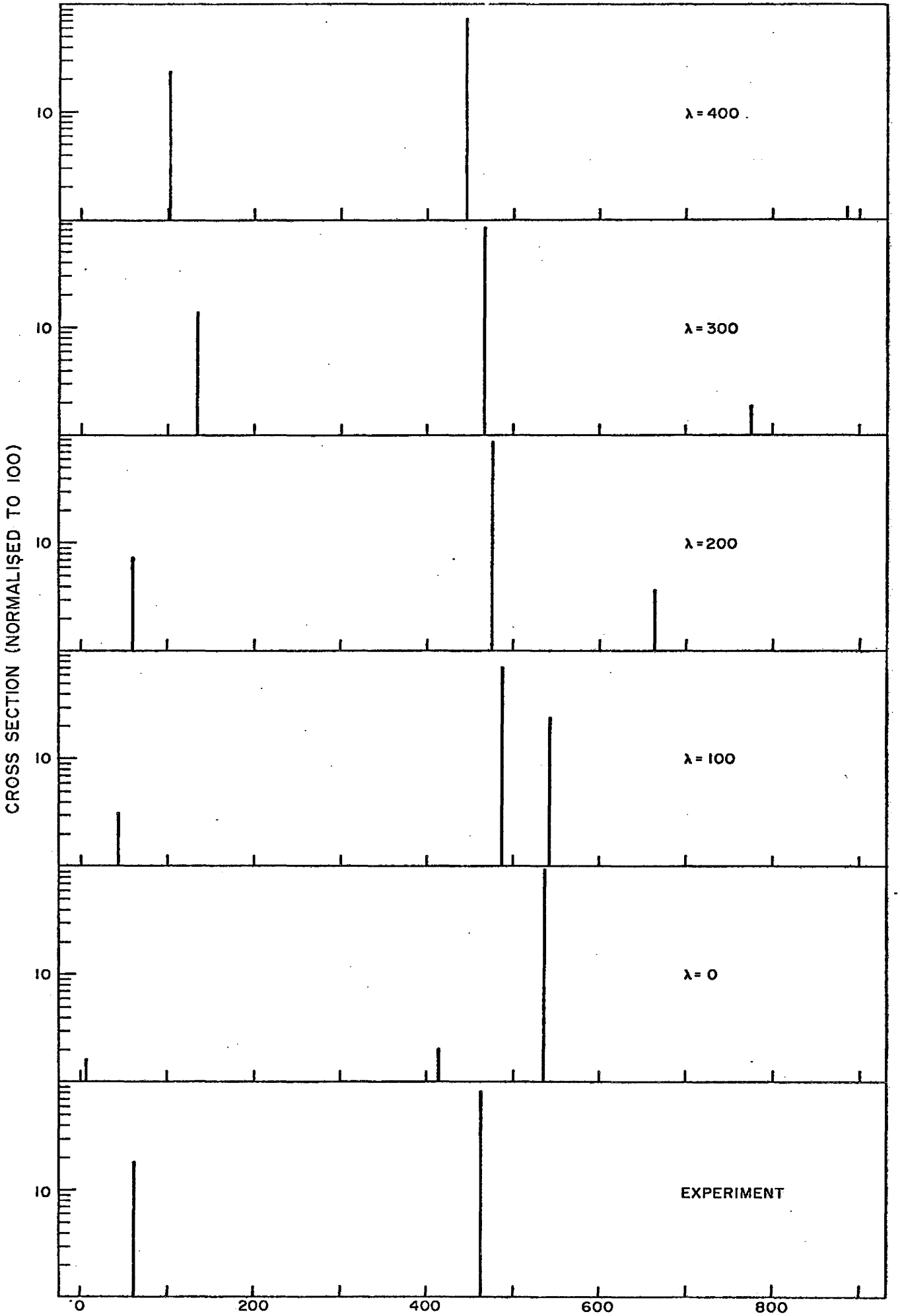
CROSS SECTION (NORMALISED TO 100)
10
λ = 400
10
λ = 300
10
λ = 200
10
λ = 100
10
λ = 0
10
EXPERIMENT
0
200
400
600
800

Fig. 4.2

Variation of the level structure of the mixed positive parity band with Fermi level. The level structure on the right was found experimentally. The arrow at A indicates the Fermi energy for the best fit to the experimental energies while the arrow at B indicates the Fermi energy which compares best with the cross section ratio of the 7/2+ states.

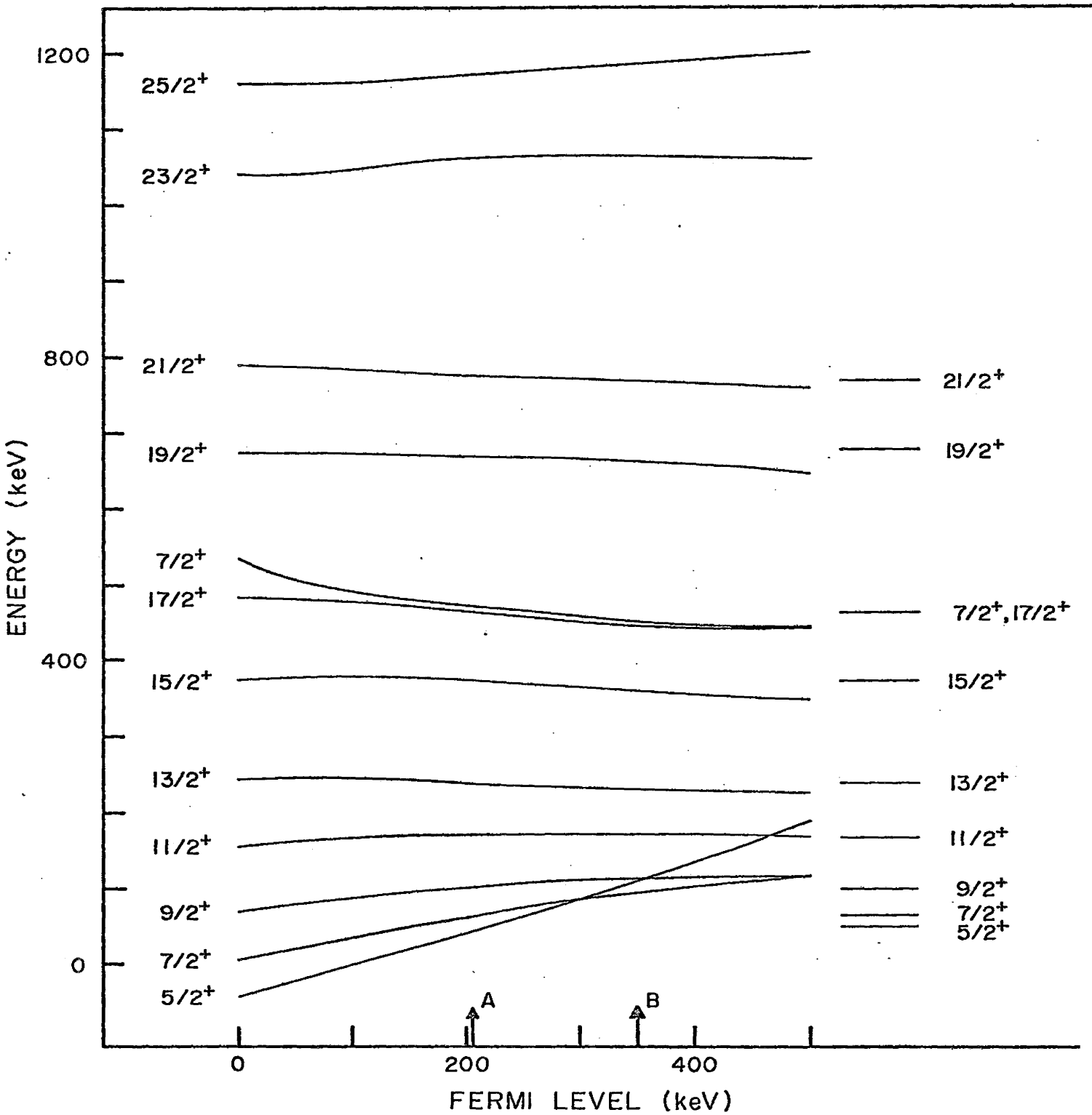
1200
800
400
0
ENERGY (keV)
25/2+
23/2+
21/2+
19/2+
7/2+
17/2+
15/2+
13/2+
11/2+
9/2+
7/2+
5/2+
21/2+
19/2+
7/2+, 17/2+
15/2+
13/2+
11/2+
9/2+
7/2+
5/2+
A
B
0
200
400
FERMI LEVEL (keV)

not been included in the calculation might be significant.

As explained previously, in this experiment the $\ell=0$ transitions were of primary importance. The main reason these particular transitions are of such interest is that of all the angular distributions in the (p,t) reaction, only the $\ell=0$ transition has constantly recognizable characteristics. Depending on beam energy and Q-value the $\ell=0$ angular distributions have minima at approximately 10° to 15° and 40° to 45° scattering angle while having maxima at about 25° and 55°.The shapes of angular distributions for $\ell\neq0$ transitions are not constant. (Elze et al. 1972 and McLatchie et al. 1970). Thus, in an experiment of this type only states which are populated by $\ell=0$ transitions can be positively identified.

For a pure $\ell=0$ transition the maximum at 25° of the angular distribution should be at least an order of magnitude greater in intensity than the minimum at 45°. A good example of this is the distribution of the $\ell=0$ population of the ground state of the ^{164}Er impurity (Figure 3.4). Now, the angular distributions of the 63 and 465 keV states have definite minima and maxima at the proper angles for an $\ell=0$ transition but they lack a sufficiently deep minimum at 40°. By comparing the minimum of a pure $\ell=0$ distribution and the minima in the distributions of the 63 and 465 KeV states, there may be about a 30% contribution from $\ell\neq0$ processes.

It appears then that $\ell \neq 0$ transitions are contributing to the population process of these states which is interesting because in previous work with the (p,t) reaction the $\ell=0$ transitions had no significant $\ell \neq 0$ transition interference. As an example, in the work done by Gadsby et al. 1973 on $^{147,149}Sm$, all of the $\ell=0$ distributions have very distinct $\ell=0$ shapes with deep minima.

In figure 3.5, the shape of the angular distributions of the 98 and 168 keV states differ from that of the 47 keV state, even though the reaction mechanism populating these final states is similar. The reason for the difference in shape may be found in the different second order processes that might populate these states (Burke and Waddington 1973; and Asciutto et al. 1972). Population could be by a) an inelastic excitation of the target followed by an $\ell=0$ transition to the final state, b) an $\ell=0$ transition to the resultant nucleus and then an inelastic excitation to the final state, c) a direct $\ell=2$ transition or d) higher order processes (Figure 4.3). Since the 47 keV state has spin 5/2+, it can not be populated by the first of these processes. One would thus expect the angular distribution to be qualitatively different from the others.

4.2 Summary

The purpose of this experiment was to provide a more rigorous test for the Nilsson model modified by pairing and Coriolis coupling. For the most part only the yrast band had

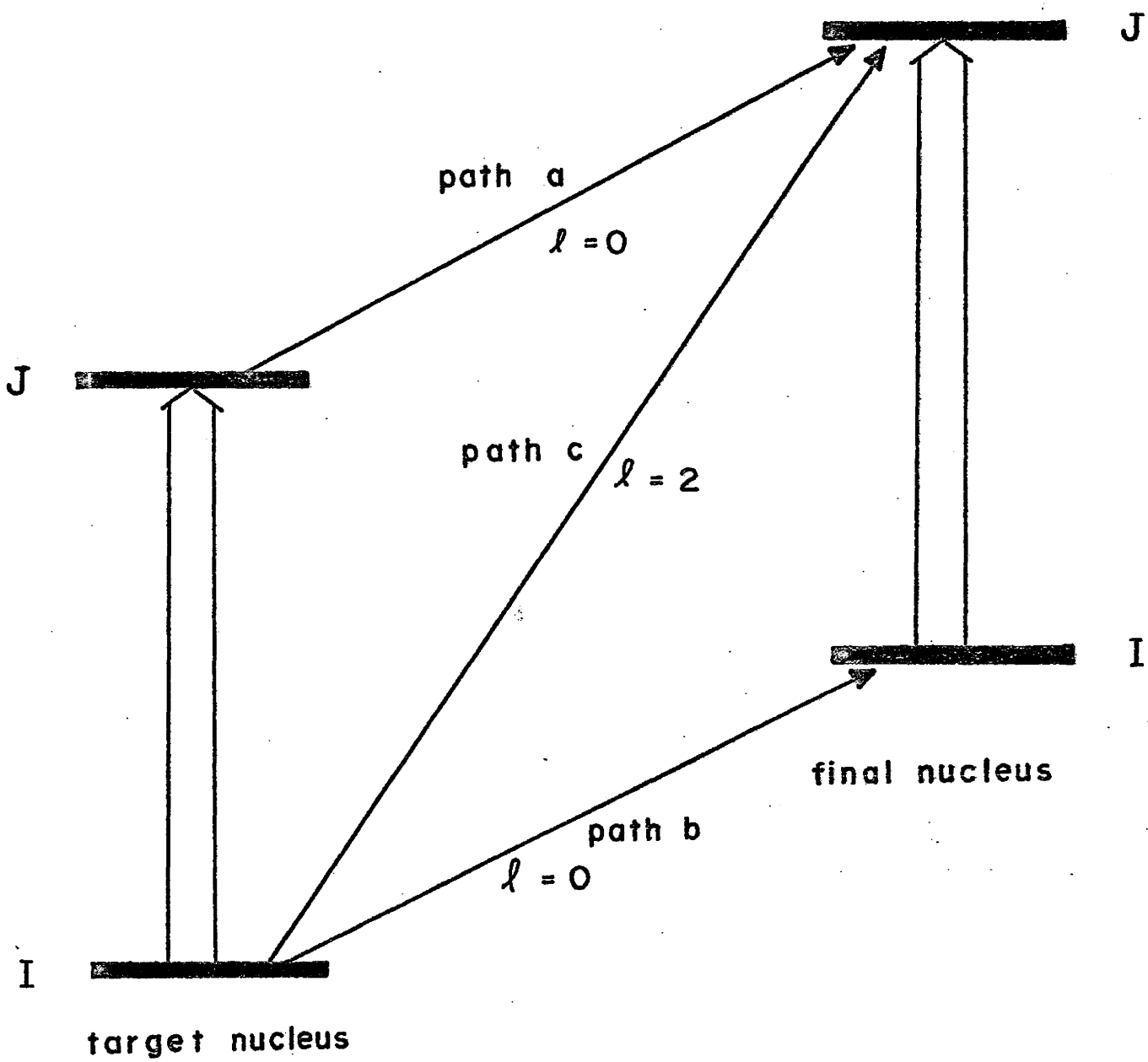

Fig. 4.3

Three of the population processes in going from the target level of spin I to the final nucleus level of spin J.

been included in previous calculations so that if higher lying band members are included a true evaluation of the model's worth can be made. Unfortunately in the present experiment only one non-yrast level's spin and parity was identified which could be included in the fitting portion of the Coriolis coupling calculation. With this included, an attempt was made to fit the known energy levels and the cross section ratio of the 7/2+ states. It has been found that this simple approach to the problem is inadequate in explaining the data.

The main conclusion resulting from this experiment is that further knowledge of level energies, spins, and parities is required to do a more sophisticated calculation. The most likely addition to the model needed to explain the data is that of the neighbouring vibrational states. If the wavefunctions of these levels were known then they could be included in the Coriolis coupling calculation. Although it was hoped that a simple explanation in terms of the Nilsson model could be found it appears that the extent of interaction among the positive parity levels forces a more complex interpretation.

REFERENCES

Ascuitto, R.J., Glendenning, Norman K. and Sorensen, B. 1971. Nucl. Phys. A183. 60.

Bardeen, J., Cooper, L.N., Schrieffer, J.R. 1957. Phys. Rev., 106, 162; 108, 1175.

Bohr, A., Mottelson, B.R. 1953. Dan. Mat. Fys. Medd., 27, 16.

Burke, D.G. and Waddington, J.C. 1972. Can. J. Phys. 50. 700.

Burke, D.G. 1974. Unpublished data.

Elze, Th. W., Boyno, J.S. and Huizenga, J.R. 1972. Nucl. Phys. A, 187, 473.

Fleming, D.G., Blam, M., Fulbright, H.W. and Robbins, J.A. 1970. Nucl. Phys. A157, 1.

Hjorth, S.A., Ryde, H., Hagemann, K.A. Løvhøiden, G. and Waddington, J.C. 1969. Nucl. Phys. A144, 513.

Kanestrom, I., Løvhøiden, G. 1971. Nucl. Phys. A160, 665.

Kunz, P.D., 1967. University of Colorado, Computer Program DWUCK, unpublished.

Løvhøiden, G., Tjom, P.O. and Edvardson, L.O. 1972. Nucl. Phys. A194, 463.

Marguier. G., Chery, R. 1972. J. Phys. (Paris) 33, 301.

McLatchie, W., Darcey. W. and Kitching, J.E. 1970. Nucl. Phys. A, 159, 615.

Meredith, J.O. and Barker, R.C. 1972. Can. J. Phys. 50, 1195.

Nilsson, S.G. 1955. Dan. Mat. Fys. Medd., 29, 16.

Oothoudt, M.A., Hintz, N.M. 1973. Nucl. Phys. A213, 221.

Preston, M.A. 1962. Physics of the Nucleus (Addison-Wesley Publishing Company Inc., Reading, Mass.).

Tjøm, P.O., Elbek, B. 1969. Mat. Fys. Medd. Dan. Vid. Selsk. 37, no. 7.